Thermal rectification in nanosized model systems: A molecular dynamics approach

Mohammad Alaghemandi,[*] Frédéric Leroy, Florian Müller-Plathe, and Michael C. Böhm

Eduard-Zintl-Institut für Anorganische und Physikalische Chemie, Technische Universität Darmstadt, Petersenstrasse 20, 64287

Darmstadt, Germany

The thermal conductivity in a set of mass-graded nanosized model systems has been studied by nonequilibrium molecular dynamics (MD) simulations in order to understand the phenomenon of thermal rectification that has been detected in externally mass-loaded nanotubes. We have found that the preferred direction of the heat transport in mass-graded nanotubes occurs from light to heavy atoms while the opposite direction of the heat transfer is observed in anharmonic mass-graded single-file chains. Mass-graded polyacetylenelike chains behave like single-file chains as long as the mass gradient is held by the backbone atoms. The thermal rectification in nanotubes with a gradient in the bond force constant (k_r) has been studied too. They are characterized by a preferred heat transfer from the region with large k_r to the domain with small k_r. Thermal rectification has been studied also in planar and three-dimensional mass-graded systems where the heat flow follows a preferred direction, similar to that observed in nanotubes. Additionally, a more realistic system has been implemented. Here, a different number of carbon nanotubes have been grafted on both sides of a graphene sheet. We have found that the transfer of the vibrational energy, as well as the generation of low-energy modes at atoms with large masses, is responsible for the sign of the thermal rectification. Its origin has been rationalized with the help of (projected) vibrational density of states. On the basis of the present MD simulations we suggest a possible design of materials showing a strong preference for the heat transfer into one direction.

I. INTRODUCTION

Rectification is a transport process that is faster in one direction than in the opposite. This phenomenon has been known for many decades for the current of charges; diodes are electric rectifiers. The first experimental papers on thermal rectification (R_t), i.e., the nonequivalence of the heat transport in two opposite directions, however, were published in 1970s. This phenomenon has been found in metal-metal and dielectric-dielectric systems.[1,2] For a current review on solid-state thermal rectification in bulk materials, we refer to Ref. 3. The recent detection of thermal rectification in externally mass-loaded carbon and boron nitride nanotubes[4] has lead to a breakthrough in nanoscience that also initiated new experimental activities on bulk materials, such as transition-metal oxides.[5] To come back to nanosized materials, the rectification effects observed here have led to an increasing interest in the physical properties of carbon nanotubes (CNTs).[6–9] Li and co-workers[10–14] have shown in a number of theoretical studies that the origin of a different heat conduction in opposite directions depends on the type of the system studied. A geometric anisotropy, for example, can be built by a conical fragment in a tube with otherwise constant diameter. Very recently such a geometric anisotropy has been studied theoretically for asymmetric graphene ribbons.[15,16] The implementation of an impurity gradient can establish a mass anisotropy. Another possibility to generate thermal rectification is the insertion of external masses at the boundaries of a low-dimensional system. Such a setup has been used in Ref. 4. The above factors are either responsible for an anisotropy in the static potential-energy surface (PES) or in the kinetic-energy part leading to a PES anisotropy in a dynamic description.[17] Modifications in the local vibrational modes yield the necessary anisotropy for the heat conduction.

In recent molecular dynamics (MD) simulations,[18] the present authors analyzed the thermal conductivity (λ) as well as the thermal conductance (σ) of CNTs as a function of the tube length (l), diameter (d), and temperature (T). This research has led to our first contact with thermal rectification in externally mass-loaded CNTs and nanotubes with a mass gradient (α).[19] However, it should be noted that a mass gradient is equivalent to a system with graded coupling constants.[20] We have found that the signs of R_t,

$$R_t = \frac{\lambda_{H \to L} - \lambda_{L \to H}}{\lambda_{L \to H}} \times 100 \ \ (\text{in} \ \%) \tag{1}$$

of mass-graded nanotubes and mass-graded one-dimensional (1D) single-file chains differ. $\lambda_{H \to L}$ symbolizes the thermal conductivity from heavy to light atoms vice versa for $\lambda_{L \to H}$. Modified definitions of thermal rectification for the mapping of other physical situations will be given in the next section. The predicted preferred heat transport in single-file chains occurs from atoms with heavy masses to light particles, leading to $R_t > 0$.[12] The negative sign of R_t calculated for nanotubes indicates that the energy transport is here more efficient when placing the light atoms at higher temperatures. In the present paper, we have adopted an R_t definition where the number of the degrees of freedom in the high and low T reservoir is identical. $R_t \neq 0$ is then caused by different efficiencies of the degrees of freedom for the transport of energy.

Differences in the physical properties of a hypothetical 1D single-file chain and nanotube models or any other quasi-1D system raise a general question. It concerns the transferability of physical concepts derived for 1D single-file chains to quasi-1D systems that are experimentally feasible. In a Brief Report,[19] we have explained why mass-graded

quasi-1D nanotubes cannot serve as a model system for perfect 1D single-file chains at least in connection with heat transport processes. The influence of anharmonicities in the potential, which are a possible prerequisite for thermal rectification, is different in mass-graded single-file chains and quasi-1D systems.

The different signs of R_t in hypothetical 1D single-file chains and quasi-1D networks such as CNTs are not unexpected. Theoretical papers emphasizing the physical peculiarities of hypothetical 1D systems have been published over many decades. More than 80 years ago, Jordan and Wigner[21] have shown that the electronic quantum statistics in single-file chains is essentially arbitrary. It differs from the conventional fermionic statistics of electronic systems that are more than one dimensional. The topology dependence of this statistics has been analyzed by one of the present authors.[22,23] Lieb and Wu[24] have demonstrated the absence of a T gradient in the interior of homogeneous single-file chains when adopting the harmonic approximation. Deviations from this behavior have been found in the framework of the Fermi-Pasta-Ulam (FPU) potential,[25] where the harmonic terms are supplemented by fourth-order coupling elements.[12] Another peculiarity of perfect 1D systems was reported by Kohn in 1950s.[26] Manifestations of the so-called Kohn anomaly, i.e., a characteristic mode softening at half band filling, on the electrical conductivity have been commented on in Refs. [27–29]. To sum up: in theoretical papers published over many decades, it has been demonstrated that the physics of single-file chains differs not only from the physics of two-(three-)dimensional (2D and 3D) materials but also from the one established in many quasi-1D systems that are experimentally accessible. Possible one-to-one correlations between the properties of hypothetical single-file chains and quasi-1D materials have become a challenging field of solid-state physics.

In the present MD study we analyze the correlation between the dimension of a system and the sign or magnitude of the thermal rectification. We have chosen nanotubes as one class of model compounds. In the past few years, it has been accepted quite generally that nanotubes are suitable models to map the physical peculiarities of 1D systems.[6–9] However, in our recent paper,[19] we have already shown that this direct correlation cannot be justified when comparing the R_t parameters of mass-graded nanotubes and 1D single-file chains. In the present contribution our recent findings will be extended in several directions. We have considered a larger collection of nanosized systems. In addition to quasi-1D nanotubes, we have studied quasi-1D chains with a polyacetylenelike structure, as well as some 2D and 3D networks. Please note that each atom in the present MD simulation has three spatial degrees of freedom (i.e., Cartesian x, y, and z coordinates) irrespective of the actual dimension of the nanosystem. The anisotropy in most of the present model systems is kinetic-energy driven as it has been generated via a mass gradient, α. For a (10,10) nanotube model we have generated a PES anisotropy via changes in the force constant under conservation of the masses. Thermal rectification under 2D conditions has been modeled for a graphene sheet with a mass gradient. Crystalline and amorphous Lennard-Jones (LJ) solids have been employed to study 3D networks. As a
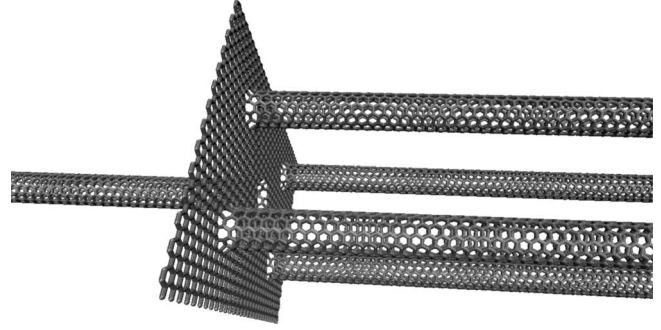
FIG. 1. Schematic picture of a (6,6) carbon nanotube rectifier where four nanotubes [right-hand side (RHS)] and a single one (LHS) are separated by a graphene interlayer.

final example, we have chosen (6,6) nanotubes in contact with a graphene interlayer that differ in the number of CNT chains on both sides of the interlayer; see Fig. 1. On one side, we have four (6,6) CNTs; on the other, only a single one. In the CNT-graphene system displayed in Fig. 1, neither the particle masses nor the force constants were modified. Here, the PES anisotropy is of purely topological origin. The systems mentioned show that we have chosen idealized models to identify key parameters for thermal rectification. Despite this simplification, our general conclusions should be transferable to real systems.

For the determination of thermal conductivities, which are a prerequisite to calculate the R_t parameters, see Eq. (1), we have adopted MD simulations of the reverse nonequilibrium (RNEMD) (Refs. [30] and [31]) and dual-thermostat (DTMD) (Ref. [32]) types. Both techniques have been used successfully in our group to derive the thermal conductivities of polymers, LJ fluids or molecular liquids.[33–37] The two methods are part of the MD program YASP which has been adopted as computational tool.[38] In Ref. [13], we have suggested that the sign of R_t in mass-graded nanotubes can be explained by a transfer of vibrational energy under the influence of anharmonicities from transverse to longitudinal modes. This transfer mechanism is more efficient when placing the light atoms at higher temperatures. Some sparse theoretical studies on mode coupling to explain heat conduction have been reported in the past decade.[39–41]

We have used the Fourier transform of the mass-weighted Cartesian velocity autocorrelation function to explain this mechanism. Up to now it does not seem to be possible to make *a priori* predictions on the preferred direction of the heat flow. The central aim of the present paper is the identification of key quantities controlling the transfer of energy in nanosized systems. On the basis of our findings we formulate some general rules on the preferred direction of the energy flow.

II. THEORETICAL TOOLS

As mentioned in the introduction, we have employed two MD techniques to derive the thermal conductivity and thus the thermal rectification of nanosized systems. Most of the simulation results have been determined by the reverse non-

equilibrium MD method.[30,31] We have adopted the dual-thermostat technique[32] only for the CNT-graphene system of Fig. 1. To calculate the thermal conductivity, we have assumed the presence of a linear T profile. Thus, we have related λ to the heat flux j_z in the direction of the T gradient, here the z direction and to the inverse of the temperature gradient $\langle dT/dz \rangle$,

$$\lambda = -j_z / \langle dT/dz \rangle. \tag{2}$$

Many years ago, it was verified theoretically[24] that such a linear T profile does not exist in perfect homogeneous 1D single-file chains when using the harmonic approximation. This restriction, however, does not occur in the studied inhomogeneous nanosized systems with their anharmonicities. They are an outcome of the coupling between the harmonic potential terms employed in our MD approach.[42] The implications of anharmonic terms on the thermal conductivity of polymeric glasses have been analyzed in a very recent study.[43] Later we come back to the role of vibrational couplings; see also the remarks in the introduction. The validity of a Fourier-type law in quasi-1D systems has been discussed critically both in experimental and theoretical papers.[44,45] Even if a linear T gradient does not exist at the chain ends, it occurs in the central part of these systems. The heat flow in the present work has been calculated only in this linear regime; again we refer to Ref. 18. Here a more detailed discussion of the shape of the temperature profile in nanotube models set into a T gradient has been given. As they are not important for the aim of the present analysis—and to save the space of the journal—such T profiles have not been commented on in the paper at hand. To reemphasize, the R_t numbers discussed below have been determined for spatial domains where a linear response is strictly valid.

As both the RNEMD and DTMD techniques have been described in the literature,[30–32] it suffices to review the basic facts. Advantages and disadvantages as well as the error bars of the methods have been described in a number of papers.[30–37] The heat flux j_z in the RNEMD method is the outcome of an artificial exchange of particle velocities in different regions. For this purpose, the system is partitioned along the z direction into equidistant slabs. One terminal slab is defined as the "hot slab" and another one as the "cold slab." At certain time intervals, the velocities of the coldest particles in the hot slab and the hottest particles in the cold one are exchanged. These swapping processes require identical masses of the respective particles. This however implies that the overall z dimension of the simulation cell for systems with a mass gradient is twice the dimension of the region characterized by a T gradient; again we refer to recent papers on the RNEMD method.[30,31] By repeating these exchange processes periodically, we can derive the heat flux j_z which offers access to the thermal conductivity λ via Eq. (2) in the steady state.

In analogy to the RNEMD method, we have two reference regions, the hot and cold one, in the DTMD technique.[32] They are locally coupled to Berendsen thermostats.[46] The temperatures in the two reference slabs are kept constant. After equilibration of the system, a linear T profile is formed in the intervening region. Parallel to the DTMD method, we

have adopted Eq. (2) to derive λ. As mentioned above, the DTMD simulations have been restricted to the CNT system portrayed in Fig. 1. To obtain a measure for the thermal rectification in this species, a modification of Eq. (1) has been necessary. The parameter R'_t in Eq. (3) guarantees that—at least technically—the same number of degrees of freedom on both sides of the graphene sheet has been taken into account. Due a drop in the temperature at the graphene interlayer, it is necessary to restrict the balance region for the heat transfer to the CNTs,

$$R'_t = \frac{j_{4 \to 1} - 4 j_{1 \to 4}}{4 j_{1 \to 4}} \times 100 \ (\text{in } \%), \tag{3}$$

$j_{4 \to 1}$ symbolizes the heat flux in the right CNT fragment with four chains toward the single chain unit on the left-hand side (LHS) under exclusion of the interlayer vice versa for $j_{1 \to 4}$.

It remains to define a thermal rectification parameter for the RNEMD simulations on the (10,10) nanotube with a constant carbon mass (12 g mol^{-1}). Here, we have generated a PES anisotropy by gradually changing the bond force constant k_r between bonded carbon atoms. The R_{tf} formula used,

$$R_{tf} = \frac{\lambda_{s \to l} - \lambda_{l \to s}}{\lambda_{l \to s}} \times 100 \ (\text{in } \%), \tag{4}$$

is a straightforward generalization of Eq. (1). $\lambda_{s \to l}$ abbreviates the thermal conductivity from the region with small bond force constants to the domain with large ones vice versa for $\lambda_{l \to s}$.

After having introduced the two MD techniques employed and the parameters describing thermal rectification, we now define the quantities chosen to explain its origin in the presence (or absence) of a mass gradient. For some nanotube systems we have calculated the power and projected power spectra by adopting the Fourier transform of the mass-weighted Cartesian velocity autocorrelation function. In the harmonic approximation, these spectra map the density of vibrational states.[47] Let us make the hypothesis that thermal rectification in mass-graded nanotubes is the outcome of an energy transfer from transversal to longitudinal modes. This coupling leads to an enhanced vibrational density of states in the longitudinal direction, i.e., in the direction of the T gradient. For recent approaches based on mode coupling we refer to the literature.[39–41] The coupling mechanism is more efficient when placing the light particles at high temperatures. The decisive role of the overlap of the vibrational spectra in the hot and cold spatial domains for thermal rectification had been mentioned already by Li *et al.*[12]

To explain the physical origin for the direction of the thermal rectification we define—in addition to the quantities R_t, R'_t, and R_{tf}—a spectral rectification parameter R_p by using (projected) power spectra,

$$R_p = \frac{P(z)_{H \to L} - P(z)_{L \to H}}{P(z)_{L \to H}} \times 100 \ (\text{in } \%). \tag{5}$$

The indices $H \to L$ and $L \to H$ have the same meaning as in Eq. (1), i.e., they indicate the direction of the heat flow in a system with a mass gradient. $P(z)$ stands for the projection of

the vibrational spectrum onto the longitudinal z direction. It is defined as

$$P(z) = \frac{\int G_Z(\omega)d\omega}{\int G(\omega)d\omega} \qquad (6)$$

with $G_z(\omega)$ abbreviating the z projection of the Fourier transform of the mass-weighted Cartesian velocity autocorrelation function $G(\omega)$,

$$G(\omega) = \frac{1}{\sqrt{2\pi}} \int_0^{t_{max}} dt e^{i\omega t} \left\langle \sum_{j=1}^{N} m_j \vec{v}_j(t) \vec{v}_j(0) \right\rangle, \qquad (7)$$

m_j stands for the mass of the jth particle and $v_j(t)$ for its velocity at time t. ω symbolizes the vibrational wave number. The Fourier transform in Eq. (7) covers the whole vibrational spectrum. t_{max} is the sampling time of the correlation function. The physical information carried by $P(z)$ can be explained as follows: as $P(z)$ represents the fraction of the total power spectrum confined to longitudinal modes, it quantifies the transfer of the total vibrational energy to this direction when the system is set into a T gradient.

At the end of this section, we want to clarify the validity and limitations of the present MD simulations. (i) The YASP force field,[38] see next section, contains—with one exception—only harmonic potential parameters for the bond lengths, angles, and torsions. Thus, we have to ask whether we can use such a potential to study a physical phenomenon that is caused by anharmonicities? Yes, we can; any coupling of harmonic potential parameters causes a certain degree of anharmonicity.[42,43] We are aware of the fact that anharmonicities are underestimated by the force field employed. Nevertheless, they are sufficient to explain thermal rectification. (ii) We have mentioned above that we have used mass-dependent particle vibrations to predict the general direction of thermal rectification. (iii) Let us dwell on the neglect of quantum effects in the present classical MD study. At the temperatures chosen, quantum effects are not decisive as they merely lead to a constant shift of all thermal conductivities.[48,49] (iv) To avoid a prohibitive computer time demand for the MD runs, we have chosen lengths of the simulation cells that are shorter than the dimensions in the micrometer range realized in experimental studies.[50–55] The length dependence of λ and σ has been studied in the recent papers.[18,56] On the basis of these results our length restriction can be justified in a study intended to explain general trends.

III. COMPUTATIONAL DETAILS

In the introduction we have already emphasized the model character of many systems adopted in the present theoretical contribution. All particles in the "carbonlike" mass-graded networks interact via a common force field, i.e., neither the harmonic force constants nor the geometrical parameters depend on the particle mass. A (10,10) nanotube model is an exception; it has been studied as a function of the bond force constant k_r. All other force constants and the respective car-
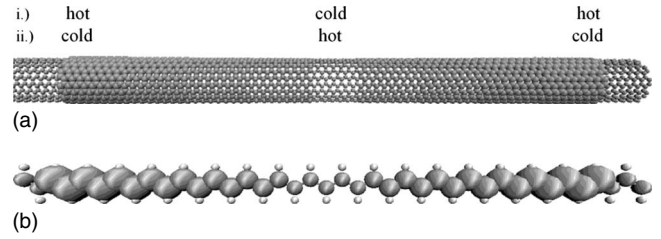
FIG. 2. (a) Schematic representation of the mass profile in the axial (z) direction of (a) a (10,10) nanotube and (b) for a polyacetylenelike topology. The chain atoms in (b) refer to effective carbon atoms, the outer ones to effective hydrogen atoms. The bigger circles represent heavier atoms. At the top of the diagram we show the two temperature profiles considered. (i) The heavy particles in both terminal regions are placed at high temperatures and the central light particles are located in the cold region. (ii) In the second T profile, the heavy particles are located in the cold terminal region while the light central particles are hot.

bon masses have been kept fixed in this series of simulations. The only model where we have chosen force constants and geometrical parameters that depend on the topology of the atoms is the 1D chain with a polyacetylenelike arrangement, where the "effective" carbon atoms are saturated by "effective" hydrogen atoms; see Fig. 2. Note that the periodic boundary conditions employed lead to a $C_n H_n$ system and not to a $C_n H_{n+2}$ one, as encountered for a system with a finite length. The descriptor effective symbolizes that we have chosen force constants and atomic increments for the bond length that are characteristic for carbon (hydrogen), even if we have modified the respective masses to introduce an anisotropy in the kinetic energy.

Although the intramolecular force field for all effective carbon systems has been optimized for CNTs, we have used the same parameters for all other carbonlike materials. This choice allowed us to restrict our analysis to the topological influence on rectification. In our study, they appear decoupled from possible modifications of the potential-energy surface due to chemical bonding.

With exception of the polyacetylene model, all quasi-1D and 2D systems studied are described by three harmonic force constants $k_r = 392\,460$ kJ mol^{-1} nm^{-2}, $k_\theta = 527$ kJ mol^{-1} rad^{-2}, and $k_\delta = 167$ kJ mol^{-1} rad^{-2} for the bond stretching, angle bending, and the dihedral behavior, respectively. The associated geometrical parameters at the PES minimum amount to $r_0 = 0.1418$ nm, $\theta_0 = 120.0°$, and $\delta_0 = 0.0°$.[57–59] The force field and geometrical parameters for the polyacetylenelike chains can be found in Table I; the data have been taken from Ref. 60. $V(\tau)$ maps the torsional behavior of the potential and k_τ is the corresponding force constant. In contrast to the dihedral term for the other networks, $V(\tau)$ is not defined by a quadratic term. For the MD simulations of the crystalline and amorphous 3D LJ solids, we have adopted $\varepsilon = 1.197$ kJ mol^{-1} and $\sigma = 0.335$ nm. These parameters have been developed for Ar.[61]

We have used the program system YASP (Ref. 38) for all MD simulations. It employs the leapfrog algorithm[62] and orthorhombic cyclic boundary conditions. They have been used for all systems irrespective of their formal dimension. Unless mentioned explicitly, the MD runs have been per-

TABLE I. Force field parameters and equilibrium values for the geometry of polyacetylene (Ref. [60]).

	$V(r) = (k_r/2)(r - r_0)^2$	
Bond	Distance/nm	k_r/kJ mol^{-1} nm^{-2}
C—C	0.1446	328668.02
C=C	0.1346	549398.71
C—H	0.1080	200000.00
	$V(\theta) = (k_\theta/2)(\theta - \theta_0)^2$	
Bond angle	θ_0/deg	k_θ/kJ mol^{-1} rad^{-2}
C—C=C	125.30	1198.36
H—C—C	116.29	505.89
H—C=C	118.41	505.89
	$V(\tau) = (k_\tau/2)[1 - \cos 3(\tau - \tau_0)]$	
Dihedral angle	τ_0/deg	k_τ/kJ mol^{-1} rad^{-2}
C—C—C—C	180.0	562.0

formed for a constant volume and temperature. Constant temperatures have been guaranteed by the Berendsen thermostat[46] with a coupling time of 1 ps. This choice rendered possible the generation of a measured mean temperature that fluctuates by less than 5 K around the target temperature. The sufficient accuracy of the thermostat has been verified in a number of test simulations. In the majority of calculations, we have chosen a target temperature of 300 K. In the 3D Lennard-Jones solid, T has been reduced to 30 K. The time step in the MD simulations is 1 fs. The nonbonded interactions, when necessary, have been determined with the help of a Verlet neighbor list, which was updated every 15 time steps. We have chosen a cutoff radius of 1.0 nm. The neighbor list cutoff exceeds this value by 0.1 nm. The particle exchange in the RNEMD simulations takes place every 300 time steps (0.3 ps). The temperature profiles have been sampled every 301 time steps. Whenever adopting this exchange period, the presence of a linear temperature gradient has been checked. A nonequilibrium simulation typically covered 6 ns. The last 2000 ps of this interval were selected for the data production. In additional test simulations over 10 ns, we have shown that 6 ns is sufficient to guarantee steady-state simulation results. This is valid for all masses and systems studied. The error bars displayed in the following diagrams always refer to the maximum value. They measure the standard deviation of the simulations.

IV. CALCULATED THERMAL RECTIFICATION PARAMETERS

A. Mass-graded nanotubes

We start the presentation of calculated thermal rectification parameters with mass-graded nanotubes of different chiral indices and tube lengths (l). The data have been derived by RNEMD simulations, which require an effective box length that exceeds the length of the domain with the T gradient by a factor of 2; see Fig. 2 for a schematic representation. The mass-graded nanotubes are generated by gradually enhancing the atomic mass along the tube axis (z). The first atoms in the nanotubes have a mass of 12 g mol^{-1}. We end with atomic masses of several hundreds. The constant mass gradient $\alpha = \Delta m(z)/\Delta z$ (in g mol^{-1} nm^{-1}) in the simulations spans a range from 1.76 to 13.76. The two combinations of the mass and temperature profile analyzed have been symbolized in Fig. 2. In this diagram, we show a (10,10) nanotube as well as a polyacetylenelike chain as representative examples. The "polyacetylene" results will be discussed in Sec. IV D. In one series of simulations, we have placed the heavy particles at the ends of the simulation box at high temperatures while the light central masses occurred in the cold region. In the second series of RNEMD simulations, the reverse combination of masses and temperatures has been studied. The symmetric mass distribution in Fig. 2 is dictated by a characteristic feature of the RNEMD technique. Note that it restricts velocity exchanges to particles of identical mass.[30,31]

The thermal rectification in nanotubes depends on a number of factors.[18,19] In Fig. 3, we have plotted R_t of nanotubes with chiral indices (5,5), (7,7), (10,10), (15,15), and (20,20) as a function of the tube diameter (d) for an average temperature of 300 K. The four curves refer to a length of 30, 50, 70, and 90 nm for the region with a mass gradient. In the whole simulation series we have adopted α = 5.76 g mol^{-1} nm^{-1}. The negative sign of R_t in Fig. 3 indicates that the preferred heat transport proceeds from the light to the heavy particles. The splitting between the four curves is enhanced with increasing tube diameter. Elongation of the tube length shifts R_t to larger negative values. For the two shorter chains, we predict an enlargement of R_t when going from the (5,5) to the (7,7) chain. This peak in the R_t curve is suppressed with an increasing length of the mass-graded re-
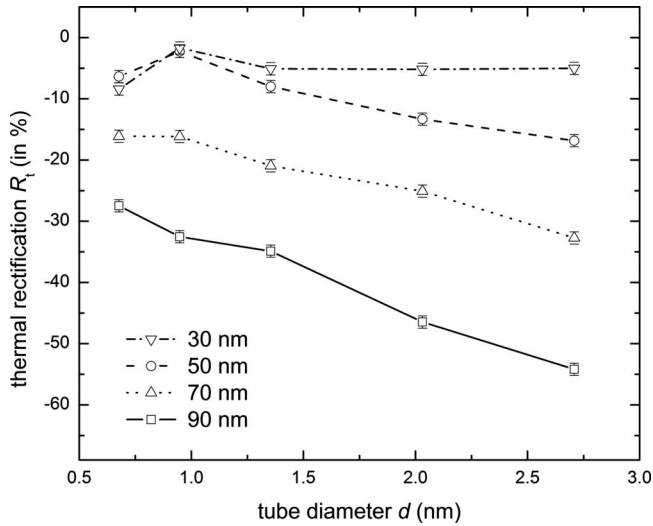
FIG. 3. Diameter dependence of the thermal rectification R_t in (5,5), (7,7), (10,10), (15,15), and (20,20) nanotubes (from left to right) with a mass-gradient length of 30, 50, 70, and 90 nm. The mass gradient α adopted in this series of RNEMD simulations amounts to 5.76 g mol^{-1} nm^{-1}. The average temperature is 300 K. In all diagrams we have plotted only the maximum error bar; see comment at the end of Sec. III. The lines in all diagrams serve only as a guide for the eye.

gion. Note that the splitting between the peak in the (7,7) system and the (5,5), (10,10) neighbors exceeds the error bars of the RNEMD approach.

In the next series of RNEMD calculations, we have studied the thermal rectification R_t in a (10,10) nanotube as a function of the mass gradient α for an effective length of 30, 50, 70, and 90 nm. The computational results have been displayed in Fig. 4. With increasing α, the parameter R_t becomes more negative. In analogy to the diameter dependence
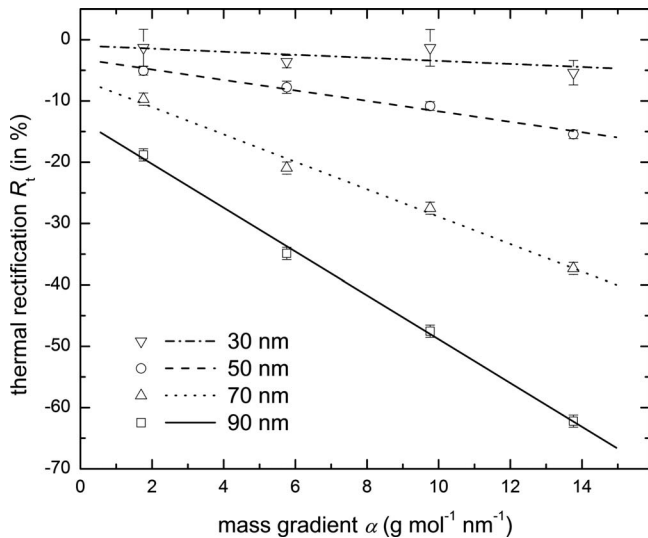
FIG. 4. Thermal rectification R_t in a (10,10) nanotube as a function of the mass gradient α. We have considered the following lengths for the mass-gradient area: 30, 50, 70, and 90 nm. The average temperature is 300 K. The data could be fitted to a straight line.

of R_t in Fig. 3, an increasing chain length causes an enhanced splitting between the curves. The thermal rectification for a mass-graded length of 30 nm depends only weakly on α. Differences in the influence of d and α on R_t become evident when comparing Figs. 3 and 4. The parameter R_t is a linear function of α with a negative slope while we have observed R_t maxima in Fig. 3 for the (7,7) nanotube as long as the length of the mass gradient is small enough ($\leq$70 nm).

The influence of the temperature on R_t has been plotted in Fig. 5. Thermal rectification in mass-graded nanotubes is reduced with increasing T. We wish to point out that this behavior has been found also for mass-graded 1D single-file chains.[12] The $T=200$ K splitting between the (10,10), (15,15), and (20,20) curves exceeds the curve splitting at 800 K by a factor larger than two. The theoretical results in Fig. 5 can be interpreted as follows. Thermal rectification profits from differences in the eigenfrequencies of the classical oscillators. With increasing T, these differences become smaller with respect to the thermal energy. The outcome of this frequency leveling is an attenuation of the thermal rectification if T is enlarged. This implies that a large selectivity for the direction of the heat transfer (i.e., large $|R_t|$) requires low temperatures. Of course, we have to keep in mind that both the force field and the restriction to the classical limit have an influence on the absolute numbers; the general trends, however, are conserved when allowing parameter changes.

FIG. 5. Temperature dependence of the thermal rectification R_t for (10,10), (15,15), and (20,20) nanotubes with an effective length of 50 nm and a mass gradient α of 5.76 g mol^{-1} nm^{-1}.

B. Nanotube simulations with a gradient in the bond force constant

Let us stay with nanotube models for a moment. The implementation of a mass gradient is not the only way to induce thermal rectification. In the following, we present RNEMD data for a (10,10) nanotube with a gradient $\beta = \Delta k_r(z)/\Delta z$ in the bond force constant k_r under conservation of a universal carbon mass of 12 g mol^{-1}. In con-
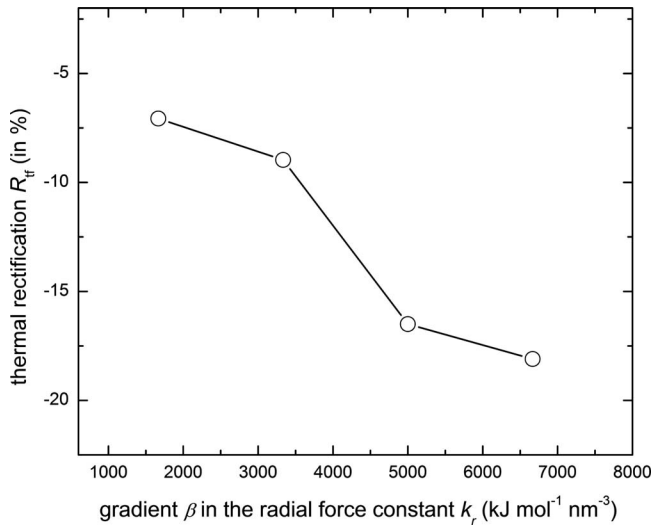
FIG. 6. Thermal rectification parameter R_{tf} in a (10,10) nanotube as a function of the gradient β in the bond force constant k_r. The RNEMD simulations have been performed for an effective chain length of 60 nm at $T = 300$ K.

trast to the implementation of a mass gradient with kinetic-energy modification, this setup yields an anisotropy in the potential energy. The two extremal β values are 1666.7 and 6666.7 kJ mol^{-1} nm^{-3}. The mean value for the bond force constant in all (10,10) chains amounts to 400 000 kJ mol^{-1} nm^{-2} which is very close to k_r adopted in the simulations of the mass-graded chains. The minimum and maximum values of k_r for the largest β value (i.e., 6666.7 kJ mol^{-1} nm^{-3}) amount to 200 000 and 600 000 kJ mol^{-1} nm^{-2}. The thermal rectification R_{tf} for systems with a gradient in the force constant has been defined in Eq. (4). Figure 6 represents the β dependence of R_{tf} for a (10,10) nanotube with an effective length of 60 nm. The simulations have been performed for an average temperature of 300 K. We predict $R_{tf} < 0$ for all β values, which indicates that the heat current in this nanochain model is more efficient from the region with large force constants to the lower k_r region. This trend is expected when remembering that the frequency of (harmonic) oscillators scales with $\sqrt{k/\mu}$, where μ denotes the reduced mass. This formula is valid both in a classical and quantum description.[62] To sum up, the local curvature of the PES is affected in the same direction when decreasing the bond force constant or increasing the reduced mass. An enhanced difference in the force constant k_r at two neighboring atoms implies a higher thermal rectification R_{tf}. The reduced efficiency for the heat transport guarantees an enhanced selectivity.

C. Mass-graded 2D and 3D models

Let us leave the nanotube models for an analysis of the thermal rectification R_t in 2D and 3D systems with a mass gradient. Recent work on 2D networks can be found in Refs. 15 and 16. We begin with a graphene sheet of 12.76 nm width and an effective length of 50 nm. The chosen width of graphene coincides almost perfectly with the circumference

of a (30,30) nanotube. The simulations summarized below have been performed for an average temperature of 300 K and a mass gradient α of 5.76 g mol^{-1} nm^{-1}. The chosen α leads to masses between 12 and 300 g mol^{-1}. The thermal rectification for the 2D graphene system has the same (negative) sign as determined in all mass-graded nanotubes. Nevertheless, it is much smaller in magnitude ($R_t = -3.7\%$) than in the (30,30) nanotube ($R_t = -17.3\%$) with the same "transversal" dimension. To explain this difference, we postulate that transversal vibrational coupling effects within a plane are less strong than transversal couplings in a bend topology like in a tube. On the one hand this coupling might find its origin in the nonzero transverse mean stress due to the tube curvature. On the other hand, this behavior is well known for quantum oscillators.[63] Thus, it seems that the present classical data fit to the results of a quantum description.

To analyze thermal rectification R_t under 3D conditions, we have chosen a Lennard-Jones solid formed by 10 000 particles in a simulation box of dimension $5 \times 5 \times 15$ nm^3. The length of the mass gradient in the z direction amounts to 6.3 nm. We have chosen $\alpha = 45.87$ g mol^{-1} nm^{-1} starting with an atomic mass of 12 and ending with 300 g mol^{-1}. The 3D system has been equilibrated at 500 K. In a sudden quenching the temperature has been reduced to 30 K to create a glass. Before starting RNEMD simulations to derive R_t, we have performed a final equilibration. The nonequilibrium run in the amorphous solid covered 1 ns. For the crystalline solid, this interval has been enlarged to 6 ns. In analogy to the mass-graded quasi-1D nanochains and graphene, we predict a more efficient energy transfer when heat flows from the light-mass to the heavy-mass region. For the amorphous LJ solid, we derive $R_t = -36.5\%$, which is reduced to -28.0% in the crystalline system. When assuming that the thermal rectification in all mass-graded systems with a dimension higher than 1D is caused by transversal vibrational couplings, it follows that this mechanism is more efficient in amorphous systems, i.e., in the absence of geometrical constraints. The enhanced selectivity (i.e., large $|R_t|$) in the amorphous system correlates with the higher λ in the crystalline material with its "undisturbed" vibrational modes.

At the end of this section, we shortly mention a possible application of the predicted mass dependence of thermal rectification. Experimentally, a mass gradient can be generated via isotopic substitution. For a recent theoretical analysis on the correlation between this substitution and thermal conductivity, we refer to the literature.[64] The implications of isotopic substitution on the thermal conductivity have been studied in a number of papers. For diamond, for example, it has been verified that λ can be reduced by 30% in samples with a random distribution of an enhanced ^{13}C concentration in the natural matrix.[65] Isotopically enriched polycrystalline diamond films have been analyzed in Ref. 66. The isotope effect on λ of silicon has been described in a conference proceeding.[67] More experimental results can be found in papers on germanium single crystals[68,69] and on the isotope effect on the thermal conductivity of boron nitride nanotubes.[70] All of these papers have shown the sensitive correlation between λ and randomly distributed isotopes. When going from a random distribution of added isotopes to a spatially ordered mass-graded one, thermal rectification is

expected. The potential of thermal rectification for the energy efficiency of buildings should become evident on the basis of our suggestion. Spatially ordered isotope substitution in windows might lead to a reduction in the heat transfer from the heated interior to the exterior.

D. Mass-graded polyacetylenelike models

In this section, we study systems with a transverse dimension smaller than in the nanotube case. For this purpose, we have chosen a mass-graded chain with a polyacetylenelike topology; see Fig. 2. Four different mass distributions (i)–(iv) have been studied. In the first series of simulations (i), the effective carbon mass has been changed linearly, whereas we have conserved the outer, i.e., hydrogen, mass which amounts to 1 g mol^{-1}. The second simulation series (ii) is characterized by a mass gradient at the outer effective hydrogen atoms while we have fixed the mass of the backbone (i.e., carbon) atoms to 12 g mol^{-1}. (iii) refers to a situation where we have adopted the same mass gradient α at the inner chain and outer atoms; its slope is identical. (iv) Finally, we have simulated a chain with opposite directions for the mass enhancement at the two types of atoms. We have adopted the same $\alpha=20$ g mol^{-1} nm^{-1} for both atomic species. This value has been conserved in all simulations described in the present section. A length of 500 nm for the polyacetylenelike arrangement has been taken throughout. Again, we have chosen an average temperature of 300 K.

The first series of simulations, i.e., mass-graded inner atoms, has led to $R_t=44.6\%$. The positive value indicates a more efficient heat transfer in the direction from the heavy inner atoms to the light ones. This direction was expected. It coincides with the findings for the 1D single-file chain described by the FPU potential.[12] The sign of R_t is dictated by the mass-graded inner part of the polyacetylenelike model while the hydrogen atoms with a constant mass do not support rectification effects. The chain model with a constant C mass and mass-graded effective hydrogen atoms (ii) reproduces the findings for the mass-graded nanotubes. The negative sign of R_t (-7.3%) indicates the influence of mass-dependent transverse couplings. The transverse vibrations arise from larger torques due to high masses at the outer atoms of the chain. The energy transfer is stronger when having the light effective hydrogen atoms at higher temperatures. When going to model chain (iii) with the same direction for the mass gradient at both types of atoms, we derive the same heat transfer as encountered in a mass-graded nanotube chain ($R_t=-28.2\%$). The enhancement of $|R_t|$ relative to the simulations of type (ii) indicates that transverse coupling effects are stronger in the absence of a large mismatch in the masses of the effective carbon atoms and hydrogen atoms. We refer to Ref. 71, where the implications of mass differences on the thermal conductivity have been analyzed. In the last simulation series (iv), with opposite directions of the two mass gradients, we reproduce again the rectification pattern in anharmonic single-file chains, i.e., R_t is positive (35.4%). Note that we have chosen a R_t definition for (iv) where R_t >0 symbolizes a preferred heat transfer from heavy carbon atoms (light hydrogen atoms) to light carbon atoms (heavy

hydrogen atoms). Under consideration of the simulations (i) and (ii), one might have expected an R_t value for the last series (iv) exceeding the R_t of model (i) with mass-graded carbon atoms. The R_t reduction from 44.6% in (i) to 35.4% in (iv), however, reflects the suppression of coupling effects with increasing mass differences within the effective C—H units; see again Ref. 71. To re-emphasize, with the mass-graded polyacetylenelike model chains, it has been possible to reproduce either the direction of the thermal rectification in 1D single-file chains (mass gradient in the central chain) or the negative R_t elements of quasi-1D nanotubes (mass gradient at the outer atoms). This possible switching in the sign of R_t gives quasi-1D systems a greater ability to model thermal conductivities than the FPU anharmonic single-file chain.

E. Topological thermal rectification

At the end of this section, we leave the analysis of idealized models and discuss the nanochain system of Fig. 1. As we have used a uniform particle mass of 12 g mol^{-1} and the same force constants within all units of the network, thermal rectification can be only of topological origin. In Sec. II, we have given the prescription to define the rectification parameter R_t', see Eq. (3), for this CNT-graphene interlayer material. Only this system has been studied by the DTMD method.[32] The temperatures of the hot and cold bath were 325 and 375 K. The T profiles for the two directions of the heat transfer are displayed in Fig. 7. In the CNT part we predict a T profile showing a rather large linearity. In the diagram this has been verified via a linear least-squares fit to the data points adopted. At the graphene interlayer, however, we have a sudden drop of T. The large temperature jump at the graphene sheet is a manifestation of a sizeable interfacial thermal resistance in the connecting region between the nanotubes and the graphene layer. A physical interpretation of this effect will be given in the next section in connection with our analysis of vibrational polarization under the influence of mode-mode coupling. Let us continue with the phenomenon of thermal rectification. For the interlayer system we have derived a topological rectification parameter, R_t', of 30.3%. From the definition of the thermal rectification in the present system, $R_t' \neq 0$ means that we have an imbalance in the thermal resistance at the graphene layer for the two directions of the heat flow. The layer-induced resistance is more important if the transferred energy is small ($1 \rightarrow 4$ direction). It is less significant for the propagation of larger energy packages. For the heat flow from the four nanotubes to a single one, the system might also benefit from interference of waves excited in the four channels.

V. ANALYSIS OF THE PROJECTED DENSITY OF VIBRATIONAL STATES—THE SPECTRAL RECTIFICATION PARAMETER R_p

As a possible step toward a microscopic explanation for the thermal rectification in the nanotube and polyacetylenelike models, we have calculated the spectral rectification parameter R_p defined in Eq. (5). Recent theoretical studies em-
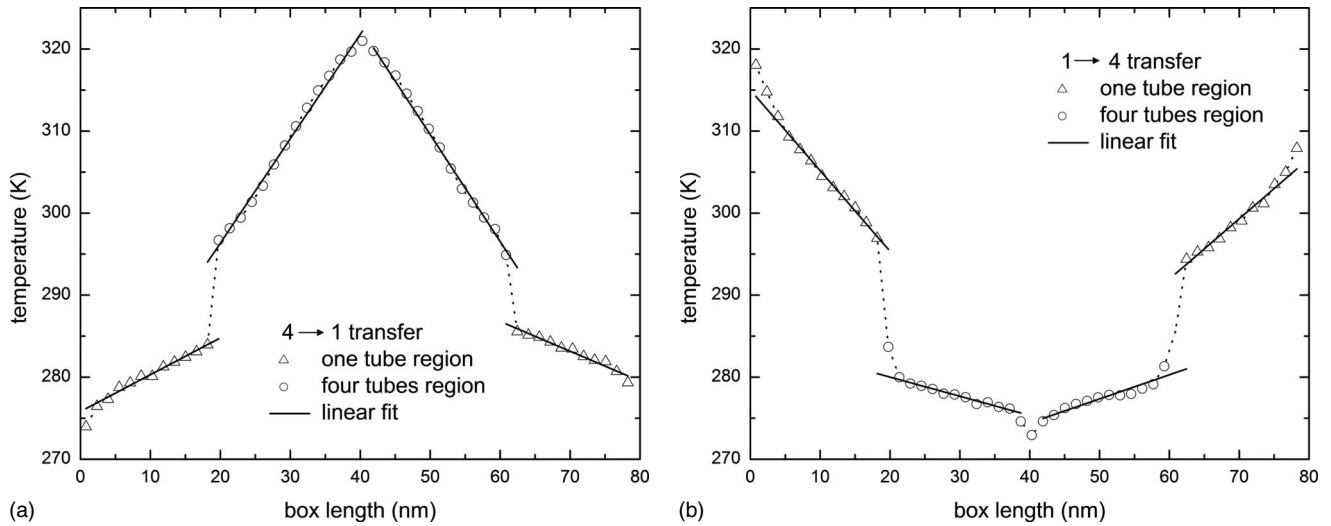
FIG. 7. Temperature profiles in the CNT-graphene system of Fig. 1 for the two different directions of the heat transfer. On the LHS, we have shown the T profile for the heat transfer from four CNTs to a single one. Vice versa for the diagram on the RHS. The slight left-right asymmetry follows from the fact that DTMD simulations require an even number of slabs in the z direction. The straight lines have been determined via a least-squares fit.

ploying the coupling between modes into different directions have been mentioned already in the introduction.[39,40] In Fig. 8, R_p is plotted for the same nanotubes as considered in Fig. 3. We have chosen an effective chain length of 50 nm and the same α as employed in the evaluation of R_t. Comparison of the two diagrams shows that the thermal rectification parameter R_t and its spectral pendant R_p are both of negative sign. Note, however, that the latter is smaller in magnitude. The $|R_t|$ and $|R_p|$ numbers become larger when enhancing the tube diameter. The local maximum of R_t for the (7,7) nanotube, however, is not reproduced by R_p. Nevertheless, we are convinced that the similarity of the two plots supports our model that thermal rectification in mass-graded nanotubes is a
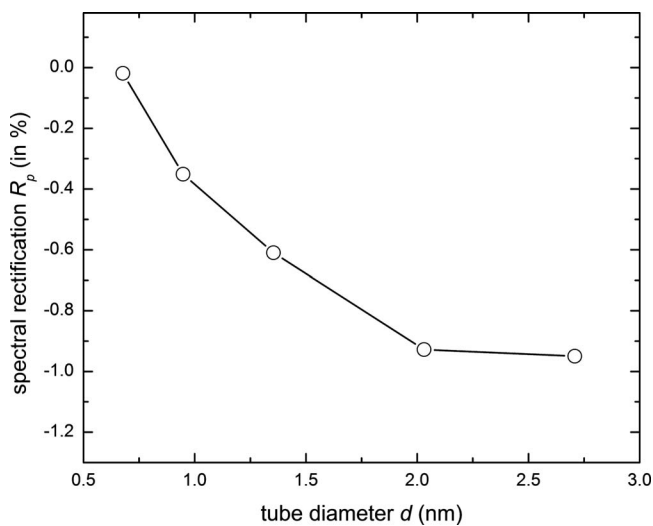
FIG. 8. Spectral rectification parameter R_p derived for (5,5), (7,7), (10,10), (15,15), and (20,20) nanotubes (from left to right) with a length of 50 nm for mass gradient and α =5.76 g mol^{-1} nm^{-1}. The average temperature is 300 K. The error bar of the simulations is smaller than the dimension of the circle.

manifestation of a polarization of the vibrational energy from the transversal to longitudinal direction. R_t (R_p)<0 implies that this mechanism is more efficient when placing the light atoms at higher T. It differs from thermal rectification in mass-graded single-file chains described by the FPU model,[12] where transversal couplings are absent. Here, the preferred direction for the energy transport profits from the fact that the excitation of light atoms by heavy ones is more efficient for a heat transfer from heavy to light atoms. The inequivalence between the two transfer paths yields $R_t>0$ in mass-graded single-file chains. The enhancement of $|R_t|$ ($|R_p|$) with increasing tube diameter in Figs. 3 and 8 simply shows that the predicted energy transfer from transversal to longitudinal modes is intensified with an increasing number of atoms, i.e., vibrational degrees of freedom. It is clear that the same argument is valid to explain the thermal rectification in the mass-graded 2D (graphenelike sheet) and the 3D models (LJ solids). Precise statements on the saturation of R_p as a function of d, as well as the origin of the local maxima in Fig. 3 would require additional (time-consuming) simulations.

Let us go to Fig. 9, where we have plotted R_p of a (10,10) CNT with a constant atomic mass of 12 g mol^{-1} as a function of the gradient β in the bond force constant k_r. In analogy to the R_t diagram in Fig. 6, the spectral rectification parameter R_p is negative and its magnitude is an increasing function of β. A physical explanation for this behavior has been given on already in Sec. IV B.

At the end of this section, let us analyze the spectral rectification R_p for the simulations (ii) and (iv) of the polyacetylenelike chain. Remember that we have derived $R_t<0$ for the model with a mass gradient at the outer atoms [i.e., for (ii)] and $R_t>0$ in the case of (iv) with opposite mass gradients at the two types of atoms. Also remember that $R_t>0$ for this example symbolizes that the preferred heat transfer goes from the heavy chain atoms (light outer atoms) to the light inner centers (heavy outer atoms). For both model studies,
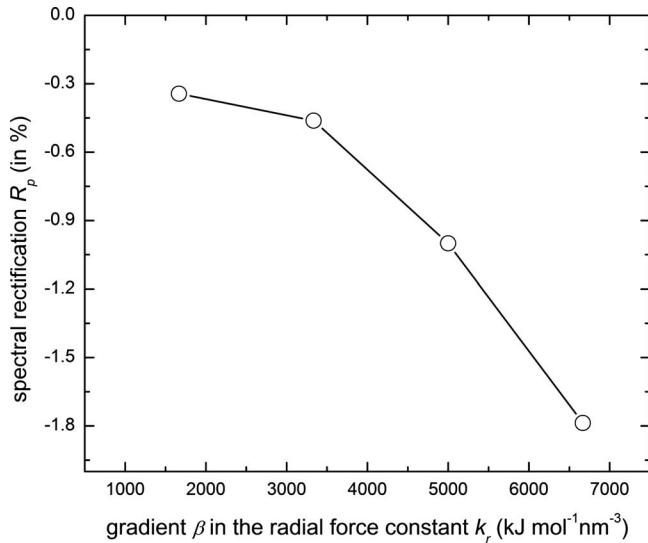
FIG. 9. Thermal rectification parameter R_p in a (10,10) nanotube as a function of the gradient β in the bond force constant k_r. The simulations have been performed at an average temperature of 300 K.

we have found that R_t and the spectral parameter R_p are of the same sign. The polyacetylenelike model (ii) can be explained by the same arguments as outlined for the mass-graded nanotubes. The energy transfer from transversal to longitudinal modes is more efficient if the transversal neighbors are light. This mechanism is operative both for neighbors that differ from the reference atoms (i.e., polyacetylene topology) and for identical neighbors (i.e., nanotubes). R_t (R_p)>0 for simulation series (iv) shows that the direction of the thermal (spectral) rectification is controlled by the mass-graded chain atoms and not by the outer ones. Again, we refer to the published data for the 1D single-file chain.[12]

On the basis of the theoretical results in this section, we are able to explain the temperature drop at the graphene interlayer in the (6,6) carbon nanotube rectifier shown in Fig. 1. The variation in the temperature as a function of the box coordinate is given in Fig. 7. The large thermal resistance at the interlayer seems to express that the vibrational transfer from the longitudinal modes in the nanotubes into the in-plane modes in the graphene layer and back is rather weak. Such a topological barrier does not exist in all other nanotubes studied. Here, each atom contributes both to transverse and longitudinal modes, which guarantees that vibrational polarization in these networks is quite efficient. The outcome of this effect has been quantified by the spectral rectification parameter R_p. We feel strongly that this is a useful quantity to explain the direction of the thermal rectification in nanosized materials. Without exception, we have found that R_t and R_p are of the same sign and of similar shape when derived as a function of model quantities, such as the tube diameter, mass gradient, or gradient in the (bond) force constant.

VI. CONCLUSIONS

In the present contribution, we have employed two MD techniques to study thermal rectification in nanosized model systems. The majority of the data have been derived by the reverse nonequilibrium MD formalism. The dual-thermostat method has been chosen to analyze the CNT-graphene interlayer model portrayed in Fig. 1. The two central topics of our theoretical work can be expressed as follows. (A) We have suggested correlation schemes to explain the direction of the thermal rectification in nanosized materials of different topologies. Thereby, we have analyzed structures ranging from a more-or-less one-dimensional boundary to 3D Lennard-Jones solids. For the design of materials with certain thermal properties, it is a prerequisite to understand the key quantities determining the transfer of heat. (B) We have adopted the flow of energy to study the transferability of physical concepts developed for 1D single-file chains to experimentally accessible low-dimensional materials. In this context, we have concisely touched theoretical contributions on different physical peculiarities of perfect 1D systems published over many decades.

Topic A. We have suggested two factors that control the direction of the thermal rectification in nanosized materials. (i) We first mention the vibrational coupling due to anharmonicities on the PES. In mass-graded nanotube models, this mechanism leads to a transfer of vibrational energy from the transversal to the longitudinal direction. The final outcome of this phenomenon is a preferred energy transfer from light to heavy particles. (ii) In mass-graded single-file chains, as well as in certain models with a polyacetylenelike topology, this coupling is either not possible or inefficient. The preferred heat transfer from heavy to light atoms in these systems can be explained by the generation of low-energy modes. For single-file chains described via the FPU potential, this mechanism has been discussed already in the literature.[12] Both for (i) and (ii), we have the situation that the present classical simulations lead to the same predictions as expected in a quantum description of the systems.[42,63] The so-called topological rectification arises from thermal resistance of the interlayer, where vibrational transfer from the longitudinal modes in the nanotube to the in-plane vibrations in the graphene layer is poorly efficient.

The detailed analysis of the different parameters controlling thermal rectification should be considered as a useful input for the design of materials with a preferred direction of heat transfer or fulfilling specific thermal requests. We have shown that thermal rectification can be induced either by the implementation of a mass gradient (isotope substitution), by a gradient in the force constants (impurity dopings), by external masses, or by modifications in the topology. All parameters lead to a modification of the mode-mode coupling in the system.

Topic B. This concerns the transferability of physical concepts that have been developed for hypothetical 1D single-file chains to real systems. At least for the transfer of energy we have quantified the conditions allowing or preventing such a correlation. In connection with thermal rectification, we have demonstrated that mass-graded nanotubes do not map the behavior of 1D mass-graded FPU chains. Such a topological discrimination is known for many physical quantities and concepts. Recent contributions of one of the present authors to this discussion have been mentioned in the introduction.[22,23,28,29] It is interesting that the topological im-

plications for thermal rectification can be related to the topology dependence of electronic quantum statistics. In quasi-1D chains, a second dimension is necessary to allow the transfer of vibrational energy from the transversal to the longitudinal direction. In quantum statistics, a second dimension is needed if electrons of the same spin should pass one another. In other words the restriction to one dimension prevents them from passing (antisymmetry constraints are not operative) and prevents the accumulation in the vibrational density of states via polarization effects ($R_t > 0$ in mass-graded single-file chains). The present data for nanotube systems with a gradient in the bond force constant, as well as the polyacetylenelike chains with different mass distributions, have led to insights into conditions allowing a correlation from the 1D boundary to experimentally accessible topologies. Again, we want to emphasize that the present analysis has been restricted to the transfer of energy. Nevertheless, we are convinced that these data are another step toward understanding the peculiar physical properties of low-dimensional materials.

We are aware of the simplifications and model assumptions that had to be accepted in the paper at hand. Despite the approximations employed, our simulations have reached the boundaries of today's computational facilities. We feel that the constraints accepted in the simulations can be justified in a theoretical model study intended to explain general trends and physical concepts. The determination of results that are accurate in an absolute sense has not been the aim of the present research.

*m.alaghemandi@theo.chemie.tu-darmstadt.de

[1] K. Balcerek and T. Tyc, Phys. Status Solidi A **47**, K125 (1978).

[2] A. Jeżowski and J. Rafalowicz, Phys. Status Solidi A **47**, 229 (1978).

[3] C. Dames, ASME J. Heat Transfer **131**, 061301 (2009).

[4] C. W. Chang, D. Okawa, A. Majumder, and A. Zettl, Science **314**, 1121 (2006).

[5] W. Kobayashi, Y. Teraoka, and I. Terasaki, Appl. Phys. Lett. **95**, 171905 (2009).

[6] R. Saito, G. Dresselhaus, and M. S. Dresselhaus, *Physical Properties of Carbon Nanotubes* (Imperial College, London, 1998).

[7] J. F. Harris, *Carbon Nanotubes and Related Structures* (Cambridge University Press, Cambridge, 1999).

[8] S. Reich, C. Thomsen, and J. Maultzsch, *Carbon Nanotubes, Basic Concepts and Physical Properties* (Wiley, Weinheim, 2004).

[9] J.-C. Charlier, X. Blasé, and S. Roche, Rev. Mod. Phys. **79**, 677 (2007).

[10] B. Li, L. Wang, and G. Casati, Phys. Rev. Lett. **93**, 184301 (2004).

[11] B. Li, J. Lan, and L. Wang, Phys. Rev. Lett. **95**, 104302 (2005).

[12] N. Yang, N. Li, L. Wang, and B. Li, Phys. Rev. B **76**, 020301 (2007).

[13] G. Wu and B. Li, Phys. Rev. B **76**, 085424 (2007).

[14] G. Wu and B. Li, J. Phys.: Condens. Matter **20**, 175211 (2008).

[15] N. Yang, G. Zhang, and B. Li, Appl. Phys. Lett. **95**, 033107 (2009).

[16] J. Hu, X. Ruan, and Y. P. Chen, Nano Lett. **9**, 2730 (2009).

[17] G. Fischer, in *Vibronic Processes in Inorganic Chemistry*, edited by C. D. Flint (Kluwer, Dordrecht, 1989), p. 7.

[18] M. Alaghemandi, E. Algaer, M. C. Böhm, and F. Müller-Plathe, Nanotechnology **20**, 115704 (2009).

[19] M. Alaghemandi, F. Leroy, E. Algaer, M. C. Böhm, and F. Müller-Plathe, Nanotechnology **21**, 075704 (2010).

[20] J. J. Xiao, K. Yakubo, and K. W. Yu, Phys. Rev. B **73**, 054201 (2006).

[21] P. Jordan and E. Z. Wigner Physik **47**, 631 (1928).

[22] J. Schütt and M. C. Böhm, Phys. Lett. A **219**, 79 (1996).

[23] M. C. Böhm and J. Schütt, Phys. Lett. A **232**, 106 (1997).

[24] E. H. Lieb and F. Y. Wu, Phys. Rev. Lett. **20**, 1445 (1968).

[25] E. Fermi, J. Pasta, and S. Ulam, http://www.physics.utah.edu/~detar/phycs6720/handouts/fpu/FermiCollectedPapers1965.pdf

[26] W. Kohn, Phys. Rev. Lett. **2**, 393 (1959).

[27] K. Dieterich and M. Wagner, Phys. Status Solidi B **127**, 715 (1985).

[28] A. G. Staib and M. C. Böhm, J. Chem. Phys. **91**, 4961 (1989).

[29] M. C. Böhm and A. Staib, Phys. Rev. B **42**, 11930 (1990).

[30] F. Müller-Plathe and P. Bordat, In *Novel Methods in Soft Matter Simulations*, Lecture Notes in Physics Vol. 640, edited by M. Karttunen, I. Vattulainen, and A. Lukkarinen (Springer, Heidelberg, 2004), p. 310.

[31] F. Müller-Plathe, J. Chem. Phys. **106**, 6082 (1997).

[32] T. Terao, E. Lussetti, and F. Müller-Plathe, Phys. Rev. E **75**, 057701 (2007).

[33] P. Bordat, D. Reith, and F. Müller-Plathe, J. Chem. Phys. **115**, 8978 (2001).

[34] M. Zhang, E. Lussetti, E. S. du Souza, and F. Müller-Plathe, J. Phys. Chem. B **109**, 15060 (2005).

[35] M. Zhang and F. Müller-Plathe, J. Chem. Phys. **123**, 124502 (2005).

[36] E. Algaer, M. Alaghemandi, M. C. Böhm, and F. Müller-Plathe, J. Phys. Chem. A **113**, 11487 (2009).

[37] E. Algaer, M. Alaghemandi, M. C. Böhm, and F. Müller-Plathe, J. Phys. Chem. B **113**, 14596 (2009).

[38] F. Müller-Plathe, Comput. Phys. Commun. **78**, 77 (1993); K. Tarmyshov and F. Müller-Plathe, J. Chem. Inf. Model. **45**, 1943 (2005).

[39] S. Lepri, Phys. Rev. E **58**, 7165 (1998).

[40] J.-S. Wang and B. Li, Phys. Rev. E **70**, 021204 (2004).

[41] J.-S. Wang and B. Li, Phys. Rev. Lett. **92**, 074302 (2004).

[42] T. López-Ciudad, R. Ramírez, J. Schütt, and M. C. Böhm, J. Chem. Phys. **119**, 4328 (2003).

[43] S. Shenogin, A. Bodapati, P. Keblinski, and A. J. H. McGaughey, J. Appl. Phys. **105**, 034906 (2009).

[44] C. W. Chang, D. Okawa, H. Garcia, A. Majumder, and A. Zettl, Phys. Rev. Lett. **101**, 075903 (2008).

[45] S. Lepri, R. Livi, and A. Politi, Phys. Rev. Lett. **78**, 1896 (1997).

[46] H. J. C. Berendsen, J. P. M. Postma, W. F. van Gunsteren, A. Di Nola, and J. R. Haak, J. Chem. Phys. **81**, 3684 (1984).

[47] H. Jobic, K. S. Smirnov, and D. Bougeard, Chem. Phys. Lett. **344**, 147 (2001).

[48] J. R. Lukes and H. Zhong, ASME J. Heat Transfer **129**, 705 (2007).

[49] J.-S. Wang, Phys. Rev. Lett. **99**, 160601 (2007).

[50] P. Kim, L. Shi, A. Majumdar, and P. L. McEuen, Phys. Rev. Lett. **87**, 215502 (2001).

[51] M. Fujii, X. Zhang, H. Xie, H. Ago, K. Takahashi, and T. Ikuta, Phys. Rev. Lett. **95**, 065502 (2005).

[52] T.-Y. Choi, D. Poulikakos, J. Tharian, and U. Sennhauser, Nano Lett. **6**, 1589 (2006).

[53] C. Yu, L. Shi, Z. Yao, D. Li, and A. Majumdar, Nano Lett. **5**, 1842 (2005).

[54] J. Hone, M. Whitney, C. Piskoti, and A. Zettl, Phys. Rev. B **59**, R2514 (1999).

[55] E. Pop, D. Mann, Q. Wang, K. Goodson, and H. Dai, Nano Lett. **6**, 96 (2006).

[56] J. Wang and J. S. Wang, Appl. Phys. Lett. **88**, 111909 (2006).

[57] C. Li and T.-W. Chou, Int. J. Solids Struct. **40**, 2487 (2003).

[58] A. K. Rappe, C. J. Casewit, K. S. Colwell, W. A. Goddard III, and W. M. Skiff, J. Am. Chem. Soc. **114**, 10024 (1992).

[59] J. H. Walther, R. Jaffe, T. Halicioglu, and P. Koumoutsakos, J. Phys. Chem. B **105**, 9980 (2001).

[60] G. Sesé and C. R. A. Catlow, Mol. Simul. **9**, 99 (1992).

[61] I. Hanasaki, A. Nakatani, and H. Kitagawa, Sci. Technol. Adv. Mater. **5**, 107 (2004).

[62] M. P. Allen and D. J. Tildesley, *Computer Simulation of Liquids* (Oxford University Press, Oxford, 1987).

[63] P. Atkins and J. de Paula, *Physical Chemistry* (Freeman, Oxford, 2006).

[64] J. Zhang and B. Li, J. Chem. Phys. **123**, 114714 (2005).

[65] D. G. Onn, A. Witek, Y. Z. Qiu, T. R. Anthony, and W. F. Banholzer, Phys. Rev. Lett. **68**, 2806 (1992).

[66] T. R. Anthony, J. L. Fleischer, J. R. Olson, and D. G. Cahill, J. Appl. Phys. **69**, 8122 (1991).

[67] A. V. Inyushkin, A. N. Taldenkov, A. M. Gibin, A. V. Gusev, and H.-J. Pohl, Phys. Stat. Solidi C **1**, 2995 (2004).

[68] V. I. Ozhogin, A. V. Inyushkin, A. N. Taldenkov, A. V. Tikhomirov, G. E. Popov, E. Haller, and K. Itoh, JETP Lett. **63**, 490 (1996).

[69] V. I. Ozhogin, N. A. Babushkina, L. M. Belova, A. P. Zhernov, E. E. Haller, and K. M. Itoh, J. Exp. Theor. Phys. **88**, 135 (1999).

[70] C. W. Chang, A. M. Fennimore, A. Afanasiev, D. Okawa, T. Ikuno, H. Garcia, D. Li, A. Majumdar, and A. Zettl, Phys. Rev. Lett. **97**, 085901 (2006).

[71] S. Maruyama, Y. Igarashi, Y. Taniguchi, and J. Shiomi, J. Therm. Sci. Technol. **1**, 138 (2006).